

FINAL REPORT

Project № UKE2-1508A-KV-05

ADVANCED METHOD OF BOUNDARY-LAYER CONTROL BASED ON LOCALIZED PLASMA GENERATION

November 2005 – May 2009

Recipients:

Institute of Hydromechanics,
National Academy of Sciences of Ukraine

Federal State Unitary Enterprise “Moscow Radio-
Technical Institute, Russian Academy of Sciences”

Authorized Secondary Collaborator:

National Aviation University of Ukraine

Partner:

European Office of Aerospace Research and Development

Report Documentation Page			Form Approved OMB No. 0704-0188		
Public reporting burden for the collection of information is estimated to average 1 hour per response, including the time for reviewing instructions, searching existing data sources, gathering and maintaining the data needed, and completing and reviewing the collection of information. Send comments regarding this burden estimate or any other aspect of this collection of information, including suggestions for reducing this burden, to Washington Headquarters Services, Directorate for Information Operations and Reports, 1215 Jefferson Davis Highway, Suite 1204, Arlington VA 22202-4302. Respondents should be aware that notwithstanding any other provision of law, no person shall be subject to a penalty for failing to comply with a collection of information if it does not display a currently valid OMB control number.					
1. REPORT DATE 15 JUN 2009		2. REPORT TYPE		3. DATES COVERED	
4. TITLE AND SUBTITLE Advanced Method of Boundary-Layer Control Based on Localized Plasma Generation			5a. CONTRACT NUMBER		
			5b. GRANT NUMBER		
			5c. PROGRAM ELEMENT NUMBER		
6. AUTHOR(S)			5d. PROJECT NUMBER		
			5e. TASK NUMBER		
			5f. WORK UNIT NUMBER		
7. PERFORMING ORGANIZATION NAME(S) AND ADDRESS(ES) National Academy of Sciences of the Ukraine, 8/4 Zheliabov St, Kiev 04057, Ukraine, , ,			8. PERFORMING ORGANIZATION REPORT NUMBER		
9. SPONSORING/MONITORING AGENCY NAME(S) AND ADDRESS(ES)			10. SPONSOR/MONITOR'S ACRONYM(S)		
			11. SPONSOR/MONITOR'S REPORT NUMBER(S)		
12. DISTRIBUTION/AVAILABILITY STATEMENT Approved for public release; distribution unlimited.					
13. SUPPLEMENTARY NOTES The original document contains color images.					
14. ABSTRACT					
15. SUBJECT TERMS					
16. SECURITY CLASSIFICATION OF:			17. LIMITATION OF ABSTRACT	18. NUMBER OF PAGES 34	19a. NAME OF RESPONSIBLE PERSON
a. REPORT unclassified	b. ABSTRACT unclassified	c. THIS PAGE unclassified			

CONTENT

Summary

Chapter I. INTRODUCTION

- Flow control concept. Background.

PROBLEM FORMULATION. BASIC TASKS:

- Part 1, AERODYNAMIC RESEARCH: flow-field response to MW discharges
- Part 2, ELECTRO-DYNAMIC RESEARCH: MW-initiated system of localized discharges
- References

Chapter II. WIND-TUNNEL COMPLEX FOR INTERDISCIPLINARY RESEARCH (WTIR), *NAU-IHM, Kiev*

SUMMARY

WIND-TUNNEL FACILITY: DESIGN, BASIC PARTS.

- Wind tunnel
- Eiffel Chamber
- Measurement and data acquisition/processing system
- Side-wall 3-component strain gage balance
- Angle-of-attack drive
- Plasma generation (or MW-heating) system:

MW generation and protection, MW system adjustment to the wind-tunnel, pulse mode of the MW system

TESTING OF THE WIND-TUNNEL SYSTEMS

- Weight testing procedure under conditions of MW radiation
- Flow-field studies
- Reference measurements in the wind tunnel (without plasma generation):

weight testing of a reference model, reference pressure measurements, validation of experiments, wind-tunnel testing of the microwave / plasma generation system, preliminary assessment of energy required for the localized plasma generation

Chapter III. PROTOTYPE INVESTIGATIONS. DESIGN OF PLASMA-CONTROLLED MODELS. FINALIZING OPTIMAZTION OF WIND-TUNNEL SYSTEMS , *NAU-IHM, Kiev*

- Reference/prototype measurements of the resistively heated model
- Design and fabrication of test models with plasma initiators
- Manufacturing of drained models with mounted pressure probes for local pressure measurements.

- Size and geometry of plasma initiators
- Summary and test models used in the finalizing experiments
- Finalized adjustments of electrodynamic and multi-initiator systems to wind-tunnel experimental conditions: *MRTI-IHM-NAU, Kiev*
 - Optimization of the electrodynamic system, *MRTI*
 - Airfoil test model for a full-scale aerodynamic experiment, *MRTI*
 - Microwave system modernization in the wind tunnel, *IHM-NAU-MRTI*
 - MW-system operation, *IHM-NAU-MRTI*
 - Implementation of the atmosphere Monitoring System, *IHM-NAU-MRTI*

Chapter IV. EXPERIMENTAL INVESTIGATIONS OF SINGLE AND MULTIPLE MW-INITIATED DISCHARGES IN THE VICINITY OF THE SURFACE IN THE AIR FLOW, *MRTI, Moscow*

- Experimental setup
- Study of the MW discharge excitation by a single vibrator
- Effects of the MW discharge over a surface of a dielectric material
- MW surface discharge characterization:

Main spatial and time features of the MW surface discharge, Investigation of the MW surface discharge trace in the airflow

- Development of a multi-initiator model for generation of multiple MW discharges over a dielectric surface:

development of the ring-type initiator design and of a multi-initiator MW-discharge system; their tests

- Parameters and design of a microwave generator, electrodynamic and multivibrator systems for experiments in the IHM-NAU wind tunnel:

MW generator and its high-voltage pulse modulator, electrodynamic system

Chapter V. THEORY OF MW-INITIATED SYSTEM OF LOCALIZED SURFACE DISCHARGES. NUMERICAL SIMULATION AND OPTIMIZATION, *MRTI, Moscow*

- Electrodynamics of various types of MW-discharge initiators
- Problems of generation of equal-power discharges across a model span in wind-tunnel experiments
- Power release in the MW discharge system matched with the available experimental equipment
- First approximation to the electrodynamic system optimization in wind-tunnel experiments

MATCHED NUMERICAL AND EXPERIMENTAL STUDIES OF FLOW CONTROL USING LOCALIZED PLASMA DISCHARGES

Chapter VI. NUMERICAL SIMULATION OF FLOW CONTROL USING SPANWISE-REGULAR ARRAYS OF PLASMA DISCHARGES, IHM, Kiev

- Setting of the numerical problem. Numerical approach, software choice
- Analysis of the flow over a surface with a constant curvature radius in presence of high-temperature plasma sources (*Laminar and turbulent flow. Effects of a turbulence level and of the thermal source energy*)
- Numerical simulations of the flow around a test model affected by high-temperature plasma sources. Matching with parameters and possibilities of aerodynamic experiments (*Location of the plasma array downstream and normally to the model surface. Estimation of a marginal λ_z spacing of generated vortices.*)
- Modeling of a pulse mode of plasma generation in a boundary layer according to the experimental operation mode and parameters

Chapter VII. EXPERIMENTAL INVESTIGATION OF FLOW CONTROL USING SPANWISE-REGULAR ARRAYS OF PLASMA DISCHARGES, NAU-IHM, Kiev

- Reference measurements
- Basic flow parameters (*ranges of free-stream velocity, angles of attack*), control parameters and regimes of operation (*pulse duration, repetition rate, a number of spanwise discharges, their location on a model*) in wind-tunnel experiments
- Measurement of aerodynamic forces under generation of spanwise-regular discharges depending on basic flow and control parameters
- Measurement of pressure distribution around the test models with MW-initiated discharges
- Joint analysis of flow-control results (*lift, drag and pressure coefficients*). Summary

Chapter VIII. IHM–NAU–MRTI: CONCLUSIONS. PUBLICATIONS. PROSPECTS.

Summary

The project **objective** consists in *interdisciplinary investigations* aimed at the development of an advanced innovative concept of flow control based on a specially designed microwave discharge generator initiating intrinsic to flow streamwise vortices with a given scale.

PART 1 of the Project is the **aerodynamic modeling of a boundary layer** with an embedded vortical structure of a given scale generated by a system of MW discharges.

Efficiency of the flow-control concept and its potential applicability is evaluated from the matched numerical and experimental results aimed to show correlation between the turbulence structure and the aerodynamic performance of the test model.

- Turbulence characteristics in a near-wall flow region are studied numerically under conditions of localized energy sources created with MW discharges over the surface.
- Temperature and velocity fields, shear stresses, lift and drag coefficients of an airfoil model are found numerically and/or experimentally depending on the basic flow parameters.
- Obtained results are analyzed together with those on the conventional resistive heating of longitudinal strips flush-mounted in the model.
- Recommendations are developed on the method optimization depending on different control scenarios accounting for a number and locations of controlled sections over a test model.

A properly organized system of localized MW discharges is shown to affect fluid motion near a wall due to the formation and maintenance of regular vortices with a given scale. Turbulence scales are modified under the relatively low energy consumption. In its turn, it results in the improved performance of the test model. Measured values of a lift-to-drag ratio of the model display the flow control efficiency for certain sets of basic flow characteristics (free-stream velocity, model angle of attack) and control parameters (spanwise scale of generated vortices, their chordwise location, intensity and a mode of MW radiation as well as a type of the MW system itself).

PART 2 of the Project is the research related to **generation of localized MW discharges as a versatile tool for the remote flow control**. It shows the feasibility of the developed technique that enables to organize microwave (MW) discharges in aerodynamically justified patterns to stimulate and support vortical fluid motion of a given structure.

This approach being a logical continuation of the earlier studies based on the localized resistive heating of the wall (P-053 project), combine the shown efficiency of the thermal control concept with advantages of non-inertial remote plasma control. Undercritical MW-initiated discharges are advantageous due to low levels of MW radiation; their necessary localization is provided due to their attachment to initiating electrodes. Finally, undercritical and deeply undercritical MW discharges are created over radio transparent dielectric surfaces.

The following basic tasks and results are fulfilled to reach the formulated goal.

- Investigation of properties of a single localized deeply undercritical MW streamer discharge in a boundary layer: spatial and temporal evolution of the discharge thermal structure in the vicinity of the wall;
- Numerical and experimental modeling of a single- and multi-initiating discharge systems in transonic flows; design and testing of a MW discharge generator optimal for the formulated flow control task;
- Calculation and optimization of energy consumed by an array of localized discharges;
- Adjustment of the developed MW-initiating discharge system to full-scale experiments in a wind tunnel; subsequent evaluation of the method applicability to various aerodynamic situations and potential applications.

INTRODUCTION

Flow control concept

Interaction of centrifugal and viscous forces in a fluid flow around curved surfaces (like those of an airfoil or a turbine blade) provides necessary and sufficient conditions for natural formation of streamwise counter-rotating vortices even in the turbulent environment [6]. In its turn, this large-scale vortical structure defines specific mechanisms of fluid transport. It is taken as a basis for the flow-control concept which consists in the maintenance of streamwise vortices intrinsic to the boundary layers under body forces but with their space scales modified so that to influence favorably integral flow characteristics [7, 10-12].

Detailed background of the developed concept, earlier results of the P-053 Project and relevant references can be found in the 3-year Report on this project.

Briefly, basic advantages of the developed thermal flow control concept can be described as follows.

- The surface stays smooth while a control factor is turned on and off at necessary moments or modes of operation.
- The control factor intensity and character can be varied according to an operation mode and depending on a location of a controlled section over a body.
- Scales of initiated vortices can be adjusted to the body geometry body as well as depending on current flow conditions,
- Flow control can be optimized due to independently controlled sections over a surface.

Following this strategy, combinations of thermal-control parameters were found in correlation

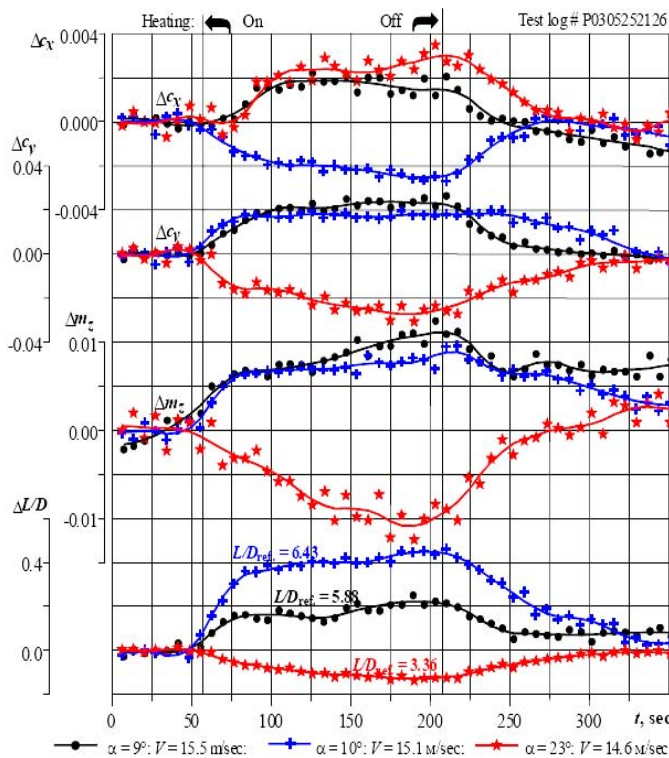


Fig. 1.1. Drag, lift, pitch moment coefficients and lift-to-drag ratio for a thermally (resistively) controlled model , $\lambda_g = 5$ mm; $\Delta T = 40^\circ\text{C}$

with basic flow parameters which improved the aerodynamic performance of a test model. It is summarized in Fig. 1 in a form of drag C_x , lift C_y , pitch moment M_z coefficients and aerodynamic quality, (Lift-to-Drag ratio) L/D , found from measured forces at different values of a free stream velocity, angles of attack and varying control factors [see Final report on P-053 project]. For the vortex scale, $\lambda_z = 5$ mm, it was found that the L/D coefficient could be raised for near-critical angles of attack.

It was shown that

- Laminar-turbulent transition was delayed from $\sim 27\%$ to $\sim 40\%$ of a model chord under controlled conditions.
- Turbulence scale modification can result in drag coefficient drop combined with the lift coefficient growth that corresponded to the lift-to-drag ratio improvement by 0.55.

Optimization of flow control within the developed “regular-vortex concept”

The temperature-driven flow control using the electrical heating of the surface (Fig. 2) is not free from disadvantages. The two basic of them are (1) inertial response (or greater characteristic times) of the overall surface-fluid dynamic system to the varying control factor and (2) smoothed $U(z)$ temperature gradients under conditions of long operation times of the activated control system.

The energy release obtained through a system of discharges within a boundary layer is free of the mentioned disadvantages. Main physical mechanisms consist in variations of fluid density and viscosity associated with temperature variations. Thus such a multidisciplinary electro- air-dynamic approach is congruent to modern flow-control strategies.

To keep the research continuity and to further raise the functionality and practicalities of the approach, Fig. 3 shows properly organized temperature fields generated with a remote method of localized plasma discharges. It makes it possible to apply the developed method, e.g., to corrosive fluids as well as to moving or rotating elements and systems, in particular, to improve

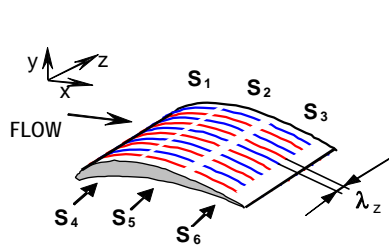


Fig. 1.2. Airfoil test model with independent resistively heated sections for the initiation of vortices with a given λ_z scale

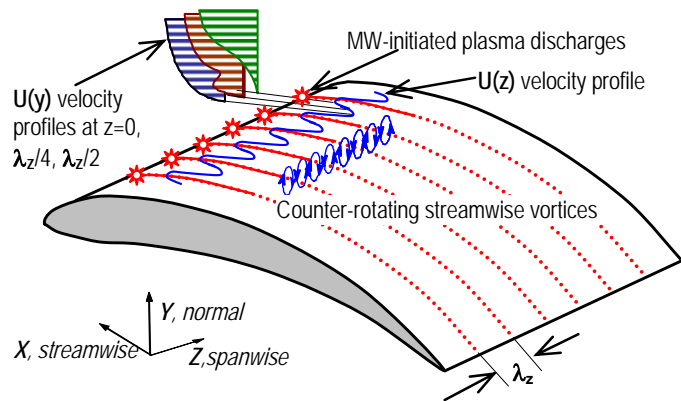


Fig. 1.3. Airfoil test model with an imposed array of plasma discharges to initiate vortices with a given λ_z scale

Figs. 1.2, 1.3. Thermally controlled test models and an illustrated impact on turbulence structure modification.

the performance of low-pressure turbine blades.

Application of the MW radiating & protection systems implies a separate electro-dynamic research related to the creation of plasma arrays with given properties. This part of the work is implemented in the partnership with a team of Moscow Radio-Technical Institute. Mechanisms of plasma-induced flow disturbances are similar to those of resistively heated surface arrays of the P-053 Project mentioned above (see Figs. 2, 3).

In case of localized plasma generation, basic control factors are the λ_z distance between the plasma actuators, amplitude characteristics corresponding to applied voltage and an operating mode of MW radiation. This kind of applied boundary conditions affects accordingly the scales and intensity of generated vortices and enables the remote control due to the MW field. In the future, the MW energy delivery to the actuators is envisaged both using an external antenna and wave-guides.

The plasma-controlled experiments required the creation of a new experimental complex aimed at measurements of aerodynamic forces under conditions of microwave radiation. A test-section of the new wind-tunnel facility was designed so that to enable experiments both with single models of airfoil- or blade-type and with turbine blade cascades.

Part 2, ELECTRO-DYNAMIC RESEARCH: MW discharge system

Here, the basic goal is to show the *feasibility to develop a technique enabling generation of localized MW discharges organized in a specified pattern in a near-wall region to initiate the fluid motion with a given space-scale*. This way, the present study combines advantages of the efficient approach based on the non-uniform resistive heating of the wall and non-inertial plasma control method.

The key issue is to develop an engineering instrument easy, reliable and flexible in operation to form a discharge pattern over a surface according to the aerodynamic requirements so that to obtain a favorable impact in a form of lift-to-drag ratio. In practice, it means

- Modeling of low-temperature plasma patches in transonic flows; design and testing of a plasma generator optimal for the formulated flow-control task.
- Properties of localized multiple electrical discharges in a boundary layer: spatial and temporal evolution of the thermal pattern in the vicinity of the wall; optimization of plasma actuator design and corresponding properties of EM fields.
- Calculation and optimization of energy consumed by an array of stable localized discharges (e.g. compared to the case of a plane discharge over a surface segment); continuous and pulse schemes of MW radiation, running and standing modes as well as versions of their experimental realizations.
- Transfer of the developed plasma-generation system to the full-scale aerodynamic experiments in the wind tunnel; prospects of this system application in other experimental facilities.

Microwave discharges applied for flow control



Fig. 1.4. Deeply undercritical discharge in a jet flow at $M=2$

Application of a MW-initiated discharges is a basis of the developed advanced method of active remote flow control. From the application viewpoint, undercritical discharges are optimal owing to low levels of MW radiation required for their maintenance [1-3]. The discharge localization is provided due to its attachment to an initiating electrode as shown in Fig. 4. Thus using a ~2 KW MW generator in a continuous or pulse mode and generating discharges as a spanwise-oriented array, one can create flow-control conditions similar to those of the spanwise-regular resistive heating of the surface.

Summarized and referenced information on types of discharges together with a certain theoretical background is given in the 3-year Report on this project. Streamer discharges are chosen for their high efficiency of interaction with the initiating EM wave.

Experiments showed that a structure and local parameters of plasma channels of the streamer discharge in its undercritical form do not change even at supersonic flow velocities [4]. The deeply undercritical discharge in a high-speed flow is usually created at a downstream (with respect to the flow) end of the vibrator when it is used as an initiator (see Fig. 4). MW energy released in this region generates an extended heated trail. Its length and width are about several millimeters and several centimeters, respectively. The temperature in the trail near the initiator is

~1,000 °C. The trail temperature and geometry substantially depend on a value of the MW power delivered to the initiator and on its design.

Undercritical and deeply undercritical MW discharges can also be initiated over a surface of a radio-transparent dielectrics [1]. In this case, physical mechanisms controlling the discharge structure and its parameters are essentially the same. Properties of the deeply undercritical MW discharge determine its applicability to the flow control near a surface [5, 10, 11]. Turn-on and off times of the control factor are of an order of a few microseconds that provides the required fast response of the control system and its low-inertia mode of operation. Operational reliability requires new engineering solutions related to the initiation of deeply undercritical streamer MW discharges organized in a specified system over the dielectric surface.

PROBLEM FORMULATION. BASIC TASKS.

Part 1, AERODYNAMIC RESEARCH: flow-field response to plasma discharges

This part combines *matched experimental and numerical studies of boundary layers developing under a temperature boundary condition formed with the localized energy release within a specific discharge pattern imposed over the surface*. It is focused on the following basic tasks.

- Design and manufacturing of a wind-tunnel facility with systems of MW generation and protection from the radiation. Design and fabrication of relevant test models equipped with the plasma actuators. Design and fabrication of a measurement complex for automated measurements of aerodynamic forces and processing of results.
- Investigation of temperature and velocity fields, shear stresses, lift and drag coefficients under vortex generation for various sets of control and basic flow parameters. Recommendations on optimal design of a system for localized plasma discharges.
- Comparative analysis of the obtained results and those known under conventional electrical heating of longitudinal strips flush-mounted in the model. Estimation of flow situations where the discharge method can be advantageous.
- Recommendations related to the method optimization using different control scenarios and its applicability to various aerodynamic problems.

The aerodynamic part of the project is implemented at the Hydromechanics Institute, National Academy of Sciences of Ukraine, and at the National Aviation University of Ukraine, both located in Kiev.

Part 2, ELECTRO-DYNAMIC RESEARCH: generation of localized MW discharges for the active remote flow control

- Investigation of properties of single and multiple localized deeply undercritical MW streamer discharges in an air flow: spatial and temporal evolution of the initiated thermal fields in the vicinity of the wall;
- Numerical and experimental modeling of multi-actuator discharge systems in transonic flows; mutual influence, resultant EM fields and their optimization to provide stable discharges; design and testing of a MW generating system optimal for the formulated flow control task;
- Calculation and optimization of energy consumed by an array of localized discharges;
- Adjustment of the developed MW-initiated plasma array to full-scale experiments in a wind tunnel; evaluation of the method applicability to various aerodynamic situations, experimental facilities and prospective applications.

REFERENCES

1. Aleksandrov, K.V., Grachev, L.P., Esakov, I.I., Khodatayev, K.V., Surface streamer MW discharge, **2002**, *J. of Engineering Physics*, v.72, No. 7, 58-62 (in Russian).
2. Grachev, L.P., Esakov, I.I., Khodatayev, K.V., **1999**, *J. of Engineering Physics*, v.69, No. 11, 19-24 (in Russian).
3. Grachev, L.P., Esakov, I.I., Mishin, G.I., Khodatayev, K.V., **1995**, *J. of Engineering Physics*, v.65, No. 5, 21-30 (in Russian).
4. Grachev, L.P., Esakov, I.I., Khodatayev, K.V. **1999**, *J. of Engineering Physics*, , v.69, No. 11, 14-18 (in Russian).
5. Esakov I.I., Bychkov V.L., Grachev L.P., Khodataev K.V. Plasma-Aerodynamic Forces Created by Microwave Discharge "Thermochemical and plasma processes in aerodynamics". *Conf. Proceedings. Saint-Petersburg 12-14 July 2004, Holding company "Leninets*.
6. Tani, I. Production of longitudinal vortices in the boundary layer along a curved wall, **1962**, *J. Geophys. Res.*, **67** (8), 3075-3080.
7. Yurchenko, N., Delfs, J., Boundary layer control over an active ribletted surface, **1999**, *In: Fluid Mechanics and its Applications*, eds. G.E.A. Meier and P.R. Viswanath, Vol.53, 217-222, Kluwer Acad. Publishers.
8. Vynogradskyy, P., Laznyuk, P., Pavlovsky, R., Zhdanov, A., "Zero Free-stream Velocity Loads Processing in Weight Tests on 6-KETV Balance in TAD-2 Wind Tunnel of KIUCA", *Herald of KIUCA*, No. 2, Kiev, 1999, (In Ukrainian).
9. Yurchenko, N., Rivir, R., Pavlovsky, R., Vinogradsky, P., Zhdanov, A., Control of the profile aerodynamics using streamwise vortices generated in a boundary layer, **2003**, *Proc. World Congress "Aviation in the XXI-st Century"*, Kyiv, Ukraine, September 14-16, 2003.
10. Yurchenko, N., Physical mechanisms of turbulence control in near-wall flows under centrifugal forces, **2007**, *37th AIAA Fluid Dynamics Conference, Miami, U.S.A.*
11. Yurchenko, N., MW-generated point plasma discharges as a novel approach to boundary-layer control, **2008**, *46th AIAA Aerospace Sciences Meeting and Exhibit, Reno, U.S.A.*
12. Yurchenko, N., Strategy of Turbulence Control Based on Flow Instability Mechanism, **2008**, *38th AIAA Fluid Dynamics and 4th Flow Control Conference, Seattle, U.S.A.*
13. Vynogradskyy, P., Yurchenko, N., Pavlovsky, R., Zhdanov, O., Aerodynamic Facility with MW-Systems for Flow Control Based on Localized Plasma Generation, **2008**, *38th AIAA Fluid Dynamics and 4th Flow Control Conference, Seattle, U.S.A.*
14. Yurchenko, N., Paramonov, Yu., Vynogradskyy, P., Pavlovsky, R., Zhdanov, O., Esakov, I., Ravaev, A., Control of flow characteristics using localized plasma discharges, **2009**, *47th AIAA Aerospace Sciences Meeting and Exhibit, Orlando, U.S.A.*

Chapter II. EXPERIMENT SUPPORT: AERODYNAMIC COMPLEX FOR INTERDISCIPLINARY RESEARCH (ACIR), KIEV

Summary.

The formulated problems of the interdisciplinary international resulted in the development of the unique experimental complex which combined the wind-tunnel facility in Kiev (Fig. 2.1) and the jet-flow unit in Moscow (Fig. 2.2). The Kiev part aims at diverse aerodynamic measurements with a possibility to work in presence of MW fields, the Moscow part is directed to test and to optimize operability of MW fields radiated around a model to control its aerodynamic performance. These complementing experimental facilities together with the involved teams of specialists in fluid dynamics and in electro-dynamics demonstrate advantages of integration of academic and educational institutions in the development of interdisciplinary international cooperation.

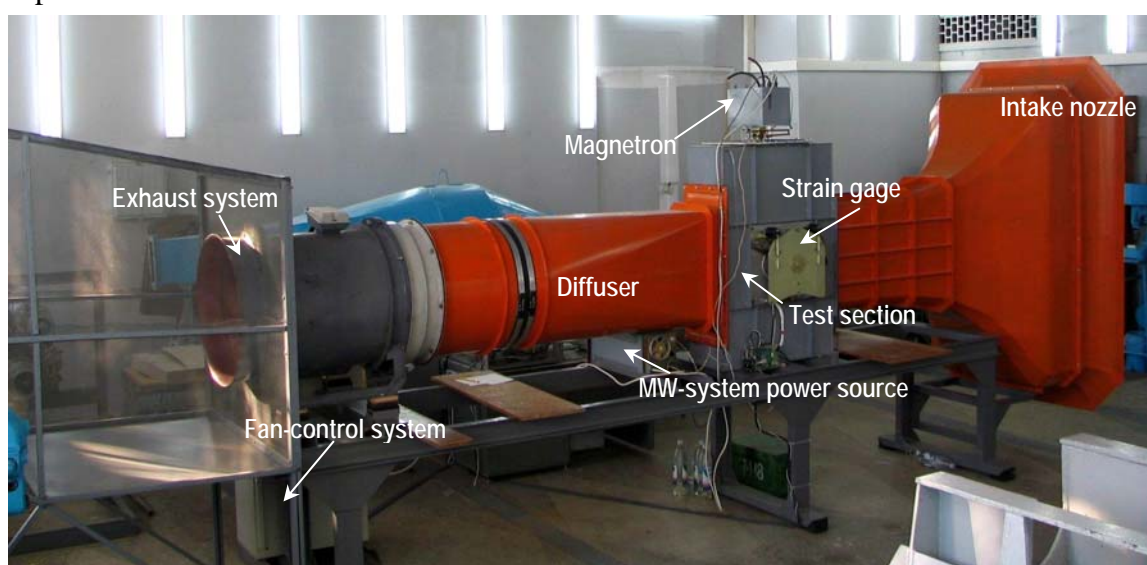


Fig. 2.1. Wind-tunnel facility equipped with the microwave-generation and protection systems to study advanced methods of flow control (Kiev)

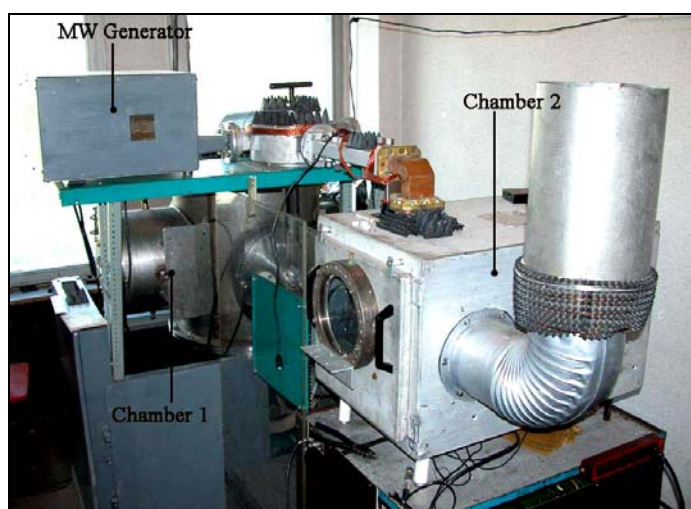


Fig. 2.2. Jet-flow facility for MW system testing (Moscow)

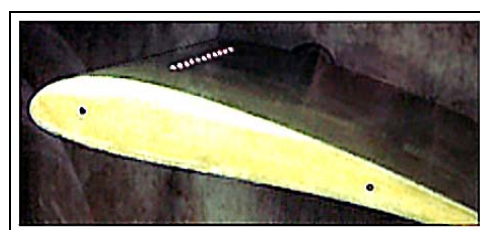


Fig. 2.1,a. The blade- (airfoil-) type model with embedded MW-initiators generating a spanwise-regular array of localized plasma discharges for experimental flow-control investigations in the wind-tunnel facility of Fig. 2.1.

Chapter II. WIND-TUNNEL FACILITY, Kiev

The following research potential and wind-tunnel parameters were envisaged at the design and development of the advanced aerodynamic complex in Kiev.

- operation in a range of free-stream velocities $U_0=0.2-50$ m/s at a low turbulence level of $\varepsilon<0.3\%$;
- classical investigations of boundary-layers over flat and curved surfaces, around test models;
- a possibility to study flows and controlled operation of turbine-blade cascades;
- flow-field measurements using two-channel hot-wire system;
- measurements of lift and drag forces to study operation of a single blade-type or airfoil-type model at various angles of attack;
- pressure measurements at selected locations over a model;
- integration of all measurement and data processing systems into a single automated complex;
- generation of microwave (MW) fields with given parameters aimed at the development of remote methods of flow control;
- adjustments of the MW generating system to experiment goals and requirements;
- protection of operators and devices from MW radiation.

BASIC HARDWARE PARTS AND CHARACTERISTICS.

Technical requirements for the wind tunnel are determined with a purpose to test single profiles and cascades with at least 200 mm span and 200 mm chord at a free-stream velocity up to 40-50 m/s at low turbulence levels. The facility provides reliable protection of personnel and electronic equipment from microwave radiation.

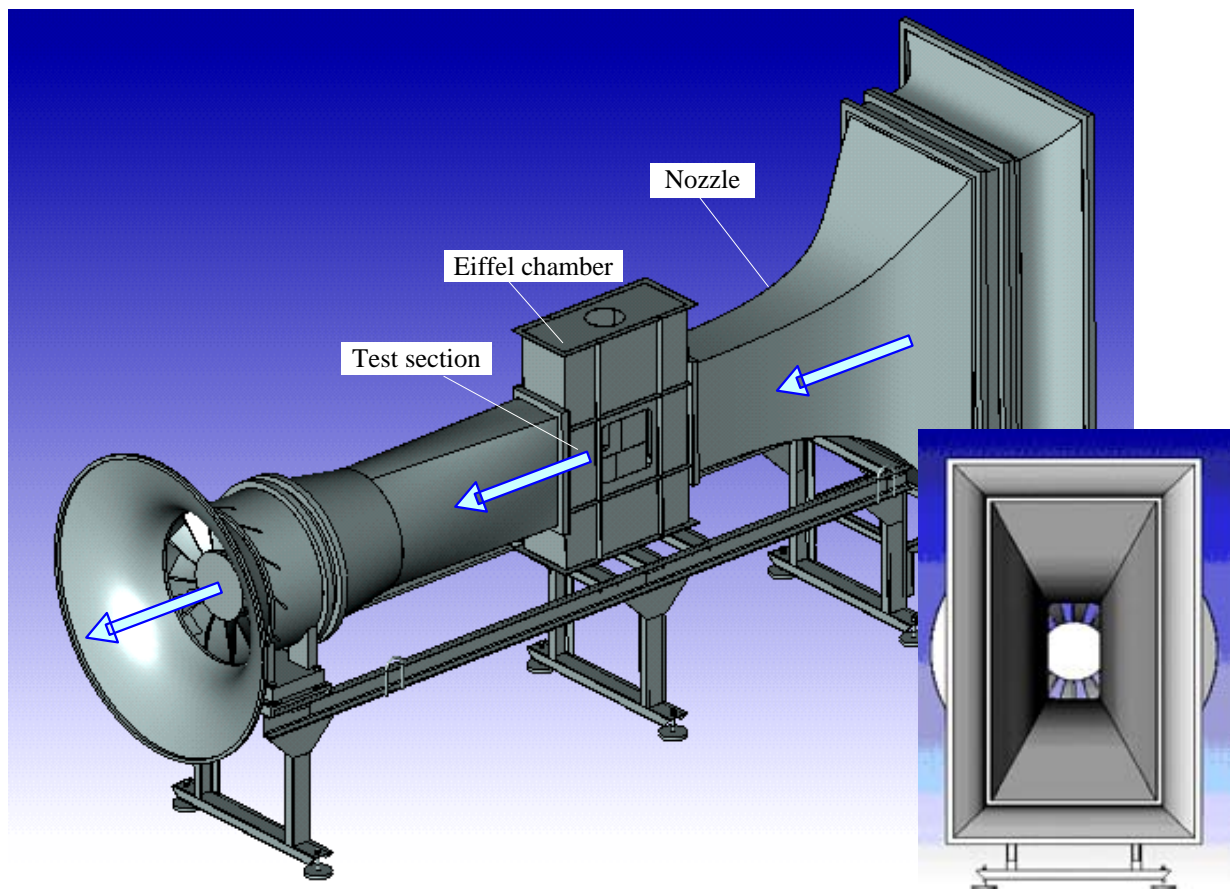


Fig. 2.3. ACIR wind-tunnel design

Detailed description of the ACIR design, its separate systems and elements, manufacturing, adjustments and testing are given in the 3-year report on the project. Basic systems and parts of the ACIR are as follows.

Wind-tunnel (Fig. 2.3) with the following specifications:

- Type: open-return.
- Material: all-metal.
- Nozzle contraction ratio: 1:10.
- Fan: 17 kW, AC-motor driven; a second fan can be installed to reach free-stream velocities above 50 m/s.
- Test section: octagonal (rectangular with cut corners) with solid sidewalls, slotted floor and ceiling, located in Eiffel chamber.
- Test section dimensions (W x H x L): 310 x 600 x 800 mm.
- Free-stream turbulence level: 0.5%.

Eiffel Chamber

The Eiffel chamber is an essential part of the wind tunnel where favorable pressure is realized. Its test section is 600 mm high and ends up with perforated walls on top and bottom. It simultaneously serves as a MW chamber with the relevant equipment installed to be outside of the airflow. These are a 3-component strain gage balance, a magnetron and MW antenna, the MW radiation absorber (on the bottom) and a window for visual observations of a model in the test section.

Angle-of-attack drive (Fig. 2.4) is used to position the model within $\pm 360^\circ$ where the angle measurement system with increment encoder ensures a position error less than 0.1° . A maximum rate of angle-of-attack variations is approximately 3 degrees per second. In addition, the measurement system with automatic angle-of-attack control is designed and installed which is based on application of a PC and the Advantech PCI-1710 multifunctional extension board.

Measurement and data acquisition/processing system (MDAS)



Fig. 2.5. Data acquisition system

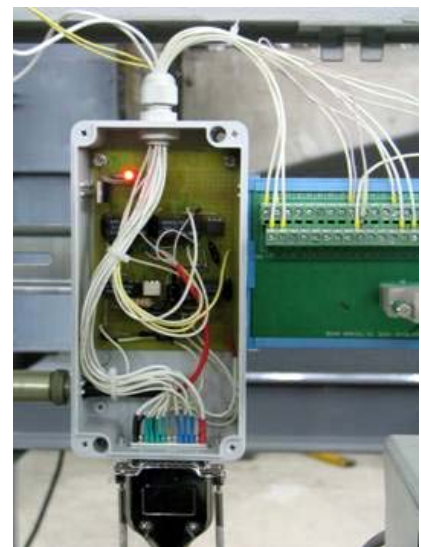


Fig. 1.4. General view of Alpha-Control Electronics Board

The **MDAS** consists of the matching hardware and software parts (Fig. 2.5). The system makes the test rig control, measurement and processing of flow parameters including noise reduction, calculation of aerodynamic coefficients, displayed test data (both text and graphic) during a test run as well as test log composition and saving information to disk.

Test rig control is the control of wind tunnel velocity (fan speed), of an angle of attack and, if necessary, of the MW-radiation module.

Side-wall 3-component strain gage balance is designed to measure lift, drag, and pitch moment within five program-controlled ranges up to 100 N for lift, 50 N for drag, and 1.8 Nm for pitch moment. Measurement errors are of order of 0.3% and the sensitivity is 0.02-0.005 N for the tested model size and available free-stream velocities.

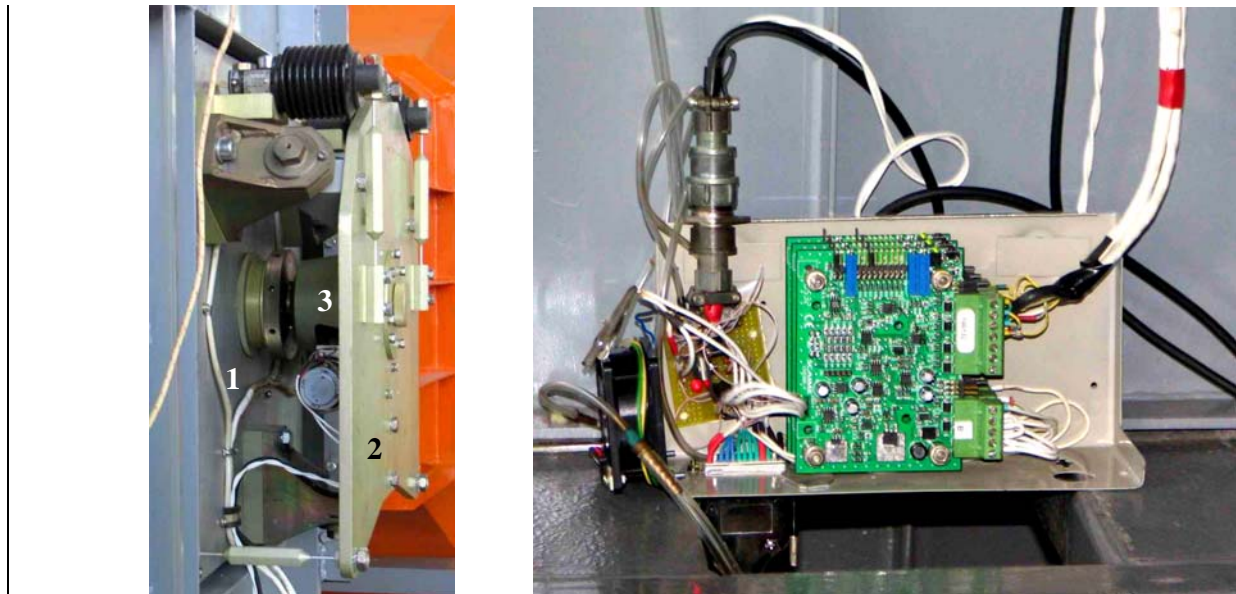


Fig. 2.6. General view of 3-component balance mounted on the test section wall (left) and its electronics (right)

The **MDAS** is designed to provide

- values of 3 components of full aerodynamic loading,
- model position relative to the free-stream direction (angle of attack),
- dynamic pressure in the test section, and other necessary parameters,
- wind tunnel and alpha-mechanism control;
- calculation of aerodynamic lift, drag, and pitch moment coefficients, dynamic pressure and Reynolds numbers within a run;
- data presentation in graphic and text formats;
- experimental data logging to the disk;
- output power of the MW system;
- up to 12 other parameters such as pressure distribution, temperature, atmospheric pressure, and humidity can also be measured simultaneously and automatically in a given mode. It enables to calculate free-stream velocity and Reynolds number. A number of measured parameters including pressure distribution around the test model can vary depending on a task.

All the details related to the design, fabrication, assemblage and testing of MDAS are given in the 3-year Project Report. In particular, they include the information about computer units controlling the operation, reduction of electromagnetic noise induced by powerful consumers such as the fan drive and the MW system, pressure measuring subsystem, determination of free-stream parameters of the WTIR and of a dynamic pressure coefficient, etc.

Maximum value of a free-stream velocity of 36 m/s was obtained at maximum ~ 2600 r/min of the axial fan. Free-stream turbulence level was roughly determined on a basis of a pressure drop along a frontal and after-body parts of a ball with a diameter of 100 mm (no more than 1%).

MW system

MW system provides an electromagnetic field with parameters necessary and sufficient for localized plasma generation in the area of a test model with a varying angles of attack. It consists of a controllable power source, the MW generator (magnetron) with a variable power, a radiating horn antenna, and, when necessary, reflecting mirrors and/or lenses. Radiated MW power can be set within 0.2-1.5 kW for continuous radiation during 0.5 s – 5 minutes. A pulse mode of radiation can be realized to provide energy necessary to initiate a spanwise set of discharges in the vicinity of the model surface. Output power can be controlled manually as well as using the data acquisition and control system. Special measures are undertaken to provide uniformity of the MW field in the area of the model displacements within the operational range of angles of attack.

MW generation control subsystem

Microwave generation is controlled by a single reconnectable digital output signal. It switches the magnetron ON to radiate a preset value of MW power. In a pulse-power mode, the signal is given to a pulse generator to the gate of high-voltage high-power transistor that switches the magnetron ON and OFF according to a pulse train. Pulse duration is typically within 0.1 - 0.3 ms, and pulse repetition rates are within 300 - 1000 Hz depending on a free-stream velocity and provided that the maximal mean generated power does not exceed 1.0 kW.

MW-protection system of ACIR

A magnetron radiates maximum MW power within a wave-guide horn to initiate a spanwise array of plasma discharges over the model surface. However partially, this power scatters around. Safe operation of the wind tunnel facility is provided due to the following measures.

1. Steel grid is installed over a whole section of the pre-chamber (Fig. 2.7). Simultaneously, this grid has an aerodynamic function to smooth the in-flow.
2. After the outlet fan collector, a rotating MW trap is mounted (Fig. 2.8). It is designed in a form of an openwork frame made from a steel grid similar to one described above which is stretched over bearing steel tubes. The system efficiency is raised using aerosol zinc metallization of grids which provides better contacts in grid nodes. Total area of the used grids at the outlet is about 8 sq m.

A significant part of MW radiation is scattered within the trap. Averaged velocity of the flow passing through the grid is less than 1 m/s.

3. A jet from an outlet fan is directed to a curved steel sheet that turns it out of the lab. This



Fig. 2.7. Entrance of a nozzle collector with the installed grid



Fig. 2.8. Fan outlet collector with the installed rotating trap

turning sheet plays a role of a MW mirror that assists scattering of MW radiation with perforated structures of the lab ceiling and walls.

4. Sealing layers made from conductive rubber sheets 3-6 mm thick are installed between flanges of all basic wind-tunnel parts.

Measurements of MW radiation around the wind tunnel proved efficiency of the developed and mounted protection system: the magnetron power of 1.5 KW creates the MW field with $\lambda_{MW} = 12.32$ cm within permitted health standards.

MW system adjustment to the wind-tunnel experiments, 1st stage

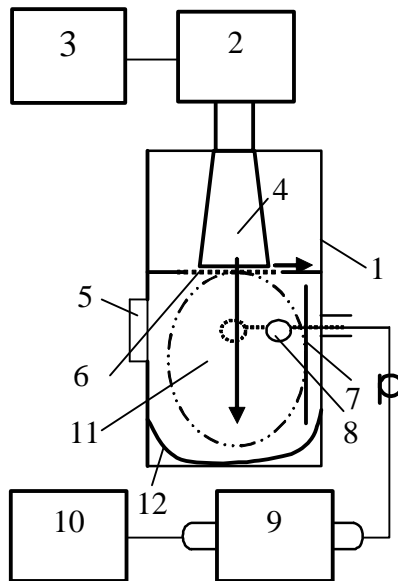


Fig. 2.9. General layout of the MW system testing

The MW plasma initiation system was initially developed and tested in MRTI in the jet-flow desktop facility with the intention to be further installed in the full-scale wind-tunnel facility in Kiev taking into account the scale effect together with real experimental conditions around the model (reflections and absorption of MW energy by the walls, MW field non-uniformity, available magnetron power, etc.).

Analysis of the MW system work conditions in the IHM-NAU wind tunnel.

Three sets of measurements of relative power level of MW radiation in the wind-tunnel test section were performed. General testing layout is shown in Fig. 2.9. Testing configuration included metal test section (1); continuous power magnetron oscillator (2); power source (3); horn antenna (4); absorbing water-filled sight port (5); metal upper wall with a radio-transparent fiberglass window (6); extruded wooden radio-absorbent side wall (7); loop coupler 14 mm diameter (8); industrial spark indicator (0.05 – 4.6 GHz) with 10 DB attenuator (9); and C1-99 oscilloscope (10). Measurements were performed in a working zone (11). Some measurements

were made with radio-absorbent water-filled vessel or rubber sheet (12) located on the lower wall of the test section.

The first set of tests gave an idea about the general power depending on high voltage values. The radiating power in the working zone without radio-absorber was found to be strongly unstable especially for greater values of supply power. The estimated radiating power of approximately 0.7 kW was insufficient to initiate plasma discharges in the wind-tunnel test section.

In two other tests, non-uniformity of radiated power was estimated in the empty test section and in presence of absorbers (water-filled plastic vessels and radio-absorbent rubber sheets). It was found that in case of the empty test section, the non-uniformity (max to min ratio) was equal to 3.3; for a concentrated load (a vessel with water), it grew up to 8.6; and for a distributed load (a sheet of rubber), it slightly dropped compared to the first case and was about 2.9. Obtained estimation enabled to formulate recommendations about coating of internal surface of the test section with the distributed radio-absorbing material. Low radiation power and considerable non-uniformity of power distribution showed that the available system with continuous MW field generation was unlikely suitable with the available low-cost magnetron to ensure reliable initiation of plasma discharges in the multi-initiator system.

Pulse mode of the MW system

A new system with considerably increased MW generator's output power in a pulse-periodic mode of operation was designed and assembled jointly with MRTI. It is described in a relevant MRTI part



Fig. 2.10. Pulse power source (covers removed)

of the 3-year Report. Fig. 2.10 shows the assembled pulse power source. Commercial 1.0 kW continuous-power air-cooled magnetron is installed and adjustable-ratio autotransformer is used to adjust a high-voltage level. G5-54 pulse generator regulates duration and a repetition rate of pulses in a wide range. Optically isolated electronic scheme was assembled and the software was accordingly modified to control magnetron on and off operation during the wind tunnel tests. The testing showed the following:

(1) the system was much more stable enabling to reliably radiate and adjust power levels in the test section;

(2) pulse power is of order of 6 kW with pulse duration within 100 - 400 μ s and a repetition rate within 30 - 200 Hz;

(3) in the worst case (of long pulses and high repetition rates), average magnetron power was much less than the rated value.

The new system was tested using the preassembled R800 model with 7 initiators, $\lambda_z=15$ mm, mounted in its axial part. MW system was switched on manually for ~ 1 s to observe plasma discharges. In the forward model position in the test section, the discharges occur over all 7 initiators. In the backward position, the discharges occur stably over 6 initiators of 7. The latter can be partly explained with the insufficient radiation power in the test section and partly, with certain power absorption by a concave surface of the model. It should be noted that the upper value of magnetron power is limited by voltage limit of an available transistor which controls pulsing power supply. This shortage can be eliminated by using a transistor with a higher voltage limit or by installing two transistors connected in a cascade. MRTI worked out the latter scheme. Such an improvement of the magnetron power source can increase the magnetron power by a factor of ~ 1.4 .

Another initiator set with 10-mm spacing, $\lambda_z=10$ mm, was fabricated and tested to approach requirements of optimal flow control for given basic flow parameters. However only several discharges were generated in this set. A set of measures was tested to improve the situation.

All the adjustment attempts and possibilities are described in detail in the 3-year Report.

TESTING OF THE WIND-TUNNEL SYSTEMS.

Weight testing procedure under conditions of MW radiation

Check-out runs were performed in the wind tunnel for the reference R800 model (i.e. the one without any control functions). Conventional weight testing procedure usually consists of two phases: (1) measurements of initial loads at zero velocity and (2) measurements in the flow.

A method of zero-velocity loads approximation was developed for a limited number of measurements within a given range of angles of attack [Vynogradskyy, P. *et al*, 1999]. It enables measurements at any arbitrary angle of attack within their range where zero-velocity loads were measured. As a result, an area of interest can be investigated in detail within the same test run. The basic procedure is universal:

1. Software program is launched and initial data are entered from the keyboard.
2. Necessary parameters for the fan control are calculated programmatically.

3. Zero velocity loads are measured in the chosen range of angles of attack, the results are approximated and coefficients are stored.
4. The program sets the model at an initial angle of attack and launches the fan.
5. Required value of a free-stream velocity is set.
6. Output signals are measured within preset time in reference conditions (MW system is OFF).
7. The MW system is ON and measurements for the controlled conditions are carried out.
8. For every sample of measured output signals, values of aerodynamic and pressure coefficients are calculated and plotted.
9. The software creates an instruction to set another angle of attack and the steps 4 through 8 are repeated until the whole range of angles of attack is covered.
10. The obtained results are logged into a hard disk as a test log file and plot a figure file.
11. If necessary, an operator can interfere into this process at any stage and change any initial data.
12. After a test run is complete, the software generates an instruction to stop the wind-tunnel drive.

Flow-field studies

For the given test-section configuration, the flow-field coefficients were determined for free-stream velocities $U_0 = 12 - 42$ m/s. Flow-field coefficient μ_q was calculated for mean values of measured pressure as follows:

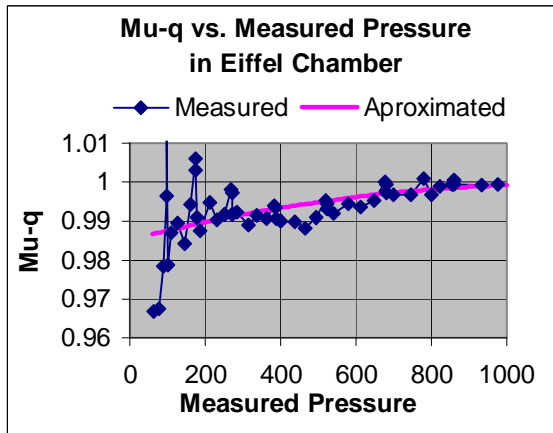


Fig. 2.11. Flow field coefficients vs measured pressure in the TAD-5 wind tunnel

$$\mu_q = \frac{\xi_{Pt} [\langle p_A - p_F \rangle - \langle p_A - p_{st} \rangle]}{(\langle p_A - p_{KE} \rangle)}, \quad (7.1)$$

where ξ_{Pt} is Pitot tube coefficient; p_A is atmospheric pressure; p_F is full (stagnation) pressure at the Pitot tube; p_{st} is static pressure at the Pitot tube; p_{EC} is the pressure at the pressure port of Eiffel chamber. Symbol $\langle \rangle$ denotes actual measured values.

Mean values of μ_q and $\langle p_A - p_{KE} \rangle$ at a given line frequency were considered to be a measurement result.

After testing, all the data were combined into one sample and for this, the approximation procedure was performed to obtain the dependence of $\mu_q = f(\langle p_A - p_{KE} \rangle)$. The 2nd order polynomial was used to approximate obtained results as shown in Fig. 2.11. Deviation (approximation error) in the range of 200 - 1000 Pa was obtained nowhere to exceed 0.5%. To reduce data scattering, more suitable pressure sensors were purchased and installed (Omega's PX291 and PX653). The approximation coefficients are used in weight testing software to calculate dynamic pressure in the test section. As far as current experimental investigations are comparative, it was found appropriate at this stage to rely upon obtained flow-field coefficients with their available accuracy.

Reference measurements in the wind tunnel (without plasma generation)

The main goal is to check repeatability of the results that would guarantee reliable measurements. It included investigations of the unit behavior, of output signals and the behavior of available devices and the developed data acquisition and control systems as well as the all-new strain gage balance. To ensure reliability of measurement results in the new IHM-NAU wind tunnel, the correlation was sought between newly obtained data and those obtained earlier in a different wind tunnel.

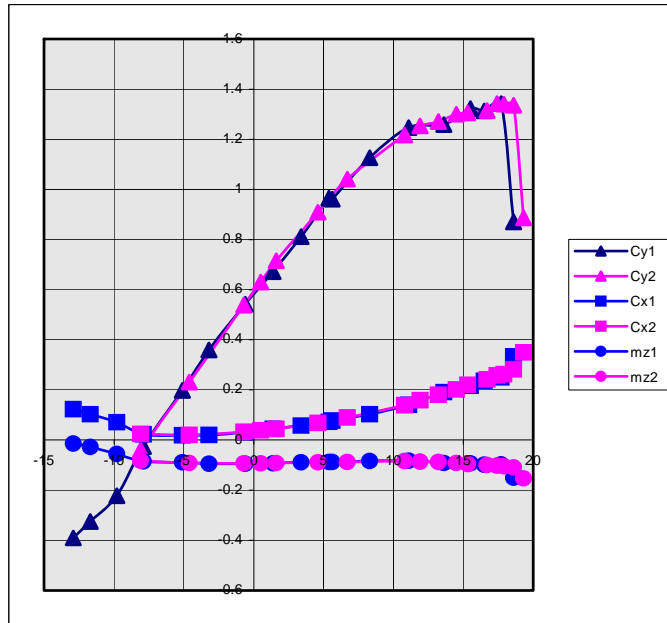


Fig. 2.12. Lift, drag and pitch moment coefficients for the reference model vs angle of attack for two different wind-tunnel facilities

Weight testing of a reference model.

Reference R800 model was used for the 5 test runs in the wind tunnel.

These tests were proceeded with an appropriate experiment preparation including earthing (to reduce data scattering), suppression of vibration-caused variation of output signals, electric noise elimination, etc. Fig. 2.12 shows good repeatability of the two sequential runs. Largest discrepancy is found for the lift coefficient. It must be an effect of flow separation which happens at different angles of attack and different Reynolds number in experiments held in different test sections with their free-stream turbulence levels.

The repeatability of drag and pitch moment coefficients is better with minute differences at near-critical angles of attack. Thus it is concluded that the new IHM-NAU wind tunnel with all-new 3-component strain gage can provide satisfactory results for the comparative weight testing.

Reference pressure measurements

A number of tests without plasma discharges was performed to develop an algorithm of simultaneous measurements of lift, drag, pitch moment, and pressure coefficients. In these tests, one of eight pressure transducers was attached to the static ports manifold of the wind tunnel nozzle to measure dynamic pressure in the test section, while other 7 probes were connected to pressure ports on the model surface. Pressure coefficients were calculated as ratios of static pressure in a particular point of the model to the dynamic pressure in the test section. Three tests were carried out in the range of angles of attack from -8° to 30° . Fig. 2.13 shows consistency and good repeatability of the measurement results, detailed discussion is given in the 3-year Report. The data obtained in spanwise triplets (ports 4, 5 & 6 and 7, 8 & 9 respectively) are sufficiently close. It drives to the conclusion that the measurement technique and the developed software enable simultaneous measurements of force/moment coefficients and pressure distribution over the model surface. Altogether, 25 test runs were made and processed within a range of -8° to $+32^\circ$ angles of attack at $U_0=10, 15, 20, 25, 30, 35$ and 40 m/s. The results of Fig. 2.13 serve as a reference basis for further flow-control investigations using the model with generated spanwise-regular plasma discharges.

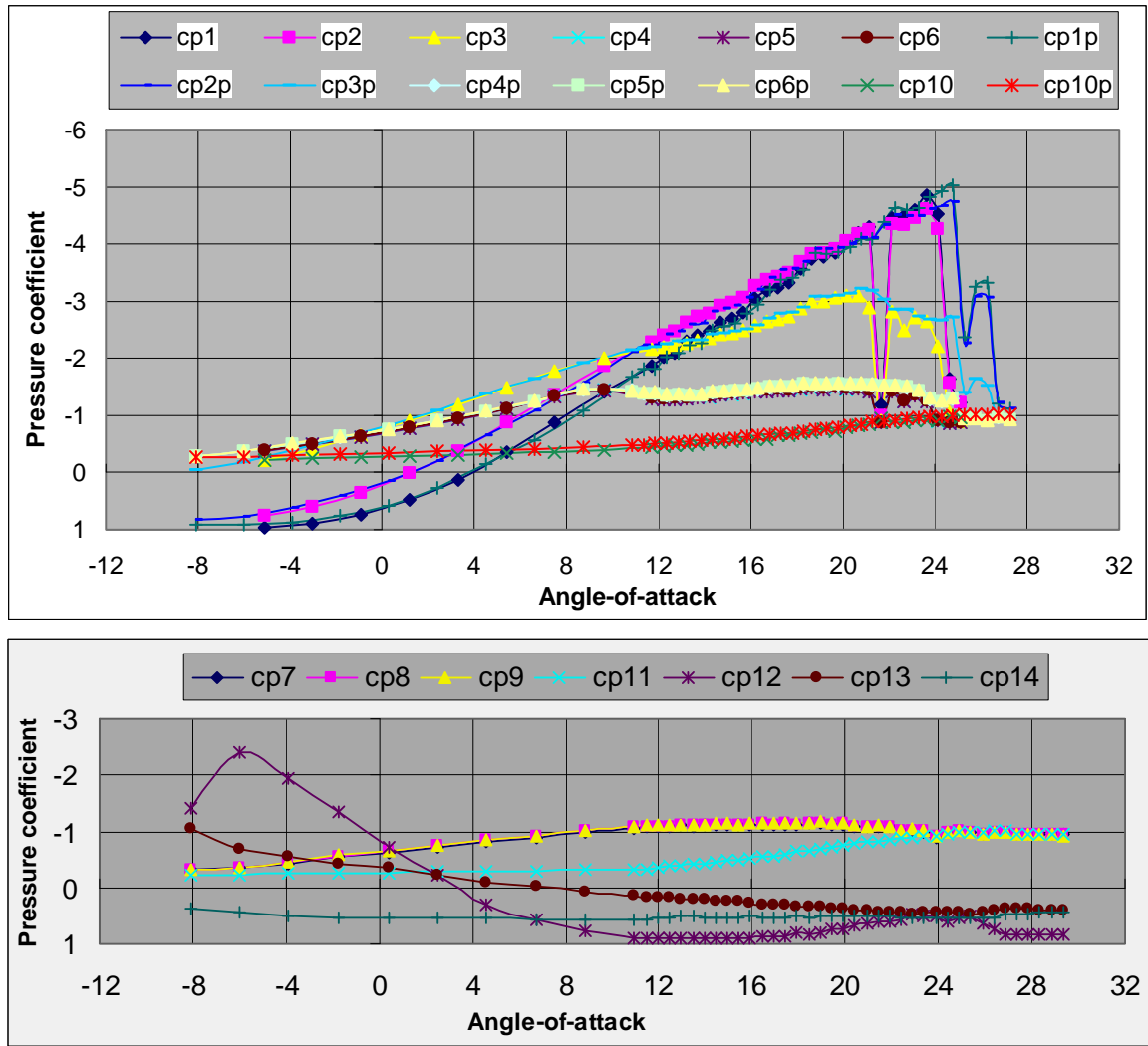


Fig. 2.13. Measured reference pressure over convex and concave walls of the model

Further validation experiments were carried out for a number of free-stream velocities using the reference R800 model without initiators. Figures 2.14 through 2.16 show. For each value of free-stream velocity, 10, 15, 20, and 25m/s, lift, drag, and pitch moment coefficients were measured depending on an angle of attack. Every data set combined over 30 wind-tunnel runs.

General behavior of all coefficients for all free-stream velocities was found to be similar up to $\alpha \sim 10^\circ$. At greater angles, drag coefficients slightly decreased with velocity increased. The stall phenomena was studied for various free-stream velocity values that was characterized with typical behavior of lift, drag and pitch moment coefficients.

Wind-tunnel testing of the microwave / plasma generation system

MW plasma initiating system was assembled on a top of the wind-tunnel test section. Several samples of a multi-initiator system were tested. In addition, a few versions of test section arrangements were analyzed in experiments including presence and absence of a radio-transparent upper wall and installation of radio-transparent or metal lower walls. It was found that a complex electromagnetic field pattern was created in the closed metal Eiffel chamber. Intensity of the electromagnetic field varied strongly at short distances that resulted in unstable generation of plasma patches.

Another problem that needed a special solution was a shape of the horn antenna which was found to be not optimal for the given facility and arrangement. Joint discussions with MRTI resulted in manufacturing of a new horn. The situation of the test section with a metal (reflecting) bottom was characterized with a standing wave with maximal electromagnetic field intensity (anti-node) in the vicinity of the multi-initiator system. At the same time, multiple reflections of running waves from the side walls interfered with this pattern and spoiled it. One of the approaches to the problem solution is to create more or less uniform electromagnetic field around initiators mounted in the model. An option is to estimate the portion of energy released in the discharges and to compare it with the energy deposited in a boundary layer of a resistively heated model in case of best flow control results obtained.

Preliminary assessment of energy required for the localized plasma generation.

Since available equipment didn't allow to obtain the MW power at the initiator system location that would be sufficient to generate stable discharges, the MW system was set to operate in a pulse mode. It supposes the application of a relatively low-power magnetron with MW radiation power of 6 to 8 kW. The pulse duration is 100 μ s, the pulse frequency is 500 or 1000 Hz. For these conditions, the duty cycle is equal correspondingly to 20 or 10.

A simple estimate gives the MW energy, $E_{MW} = 0.6-0.8$ J radiated in a pulse. Empirically, it was found that the energy released in a boundary layer in a form of the discharges (i.e. with account of a dissipated portion of the radiated energy) is approximately $E_{MW} / 10$, i.e. in our case, the energy released in a single discharge from a set of available 11 in the plasma array is $E_{BL} = (6 \text{ or } 8) \times 10^{-3} \times 0.5$ (or 1) $\times 10^{-1} = 3$ (or 8) $\times 10^{-4}$ J. That is the averaged pulse power of a single thermal source within the plasma array in experiments is roughly 3 to 8 W.

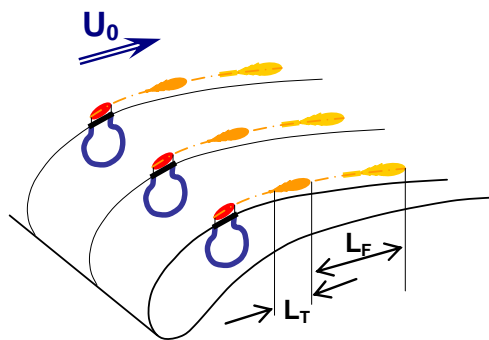


Fig. 2.14. Illustration of a thermal pattern generated in a boundary layer with plasma discharges initiated in a pulse mode

Being located at an outer part of the boundary layer, thermal sources initiated with plasma discharges travel downstream with the velocity close to the free-stream velocity, i.e. 20-30 m/s. That is at the given $U_0 = 20$ m/s and MW pulse frequency of 1000 Hz, a thermal source propagates downstream by 2 cm; under this conditions, no more than 10 thermal spots generated by one discharge can be found over a model. Each of the thermal spots is of $L_T \sim 2$ mm long in a downstream direction and is elongated losing its temperature in a process of its downstream propagation as it is illustrated by Fig. 2.14. The whole thermal pattern over a model reminds a field of heated tracer shells. Of course, one can change the frequency and duration of pulses thus changing L_T and L_F

lengths but it cannot change significantly a total energy deposited in a boundary layer. A more precise energy estimation for the case of localized plasma discharges initiated in a pulse mode of the generator is given in the MRTI part of reporting.

In any case, it is evident that the generation of stable energy-carrying discharges requires both enhancement of the MW-system efficiency for the operation in the wind tunnel and/or usage of a more powerful MW generator. Both ways are time and budget consuming, i.e. not practically realizable in the framework of one project. Therefore sophisticated "half-measures" were undertaken which were based on optimization of the pulse radiation regime and minute adjustments in the wind tunnel according to recommendations of the electro-dynamic part of the research team.

Chapter III. PROTOTYPE INVESTIGATIONS.

DESIGN OF PLASMA-CONTROLLED MODELS.

FINALIZING OPTIMIZATION OF WIND-TUNNEL SYSTEMS:

IHM-NAU, Kiev

Investigations of the model with arrays of plasma discharges proceeded from experiments with the resistively heated model. The latter tests helped to determine a location where the array should be optimally mounted as well as to get information on intermittency of heating. Thus aerodynamic requirements to the model design were developed on the basis of resistively operated thermal control as well as of recommendations regarding the MW-field organization and an electromagnetically affordable distance between the actuators (a spanwise-scale of introduced streamwise vortices).

Reference/prototype measurements of the resistively heated model

Development and preparation of the aerodynamic facility to the plasma-controlled experiments was implemented with strongly coordinated efforts of all the 3 project teams. The present project problem illustrated in Fig. 3.1 is similar but not identical to the earlier studied problem of boundary-layer control based on voltage-heated z-spaced longitudinal elements (Fig. 3.2). In addition to temperature values, plasma-generated thermal fields are essentially non-stationary under pulse MW excitation of plasma initiators.

In this connection, a series of measurements was planned with the conventional resistively heated model of Fig. 3.2 under periodic heating of thermal elements to model a pulse mode of MW-initiated thermal fields. It was intended as a prototype and reference experiment to give a basis for the formulated research task illustrated in Fig. 3.1. It is obvious that not only temperature values and fields but also time scales in these two experiments are different. However aerodynamic coefficients measured under conditions of non-stationary heating may give a better insight into the physics of the studied phenomena.

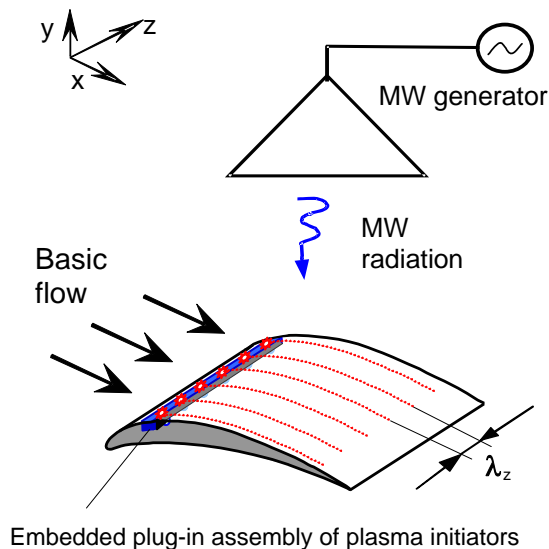


Fig. 3.1. Sketch of experiments on flow control using z-localized plasma generation in a boundary layer

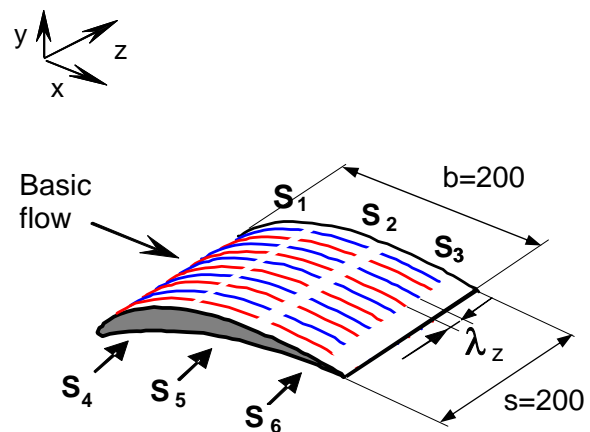


Fig. 3.2. Sketch of experiments on flow control using localized resistive heating of z-regular flush-mounted streamwise strips arranged into 6 independently controlled sections

The R800 model of Fig. 3.2 was tested at its reverse position under the 9° angle of attack to the free-stream vector. Two upstream sections were heated to provide $\lambda_z = 5$ mm with a temperature difference $\Delta T = 40^\circ$. For comparative analysis, Fig. 3.3 shows pitch moments as most sensitive aerodynamic characteristics in present experiments obtained for 6 modes of intermittent heating as well as reference results with continuous heating switched on after 40 s of aerodynamic forces

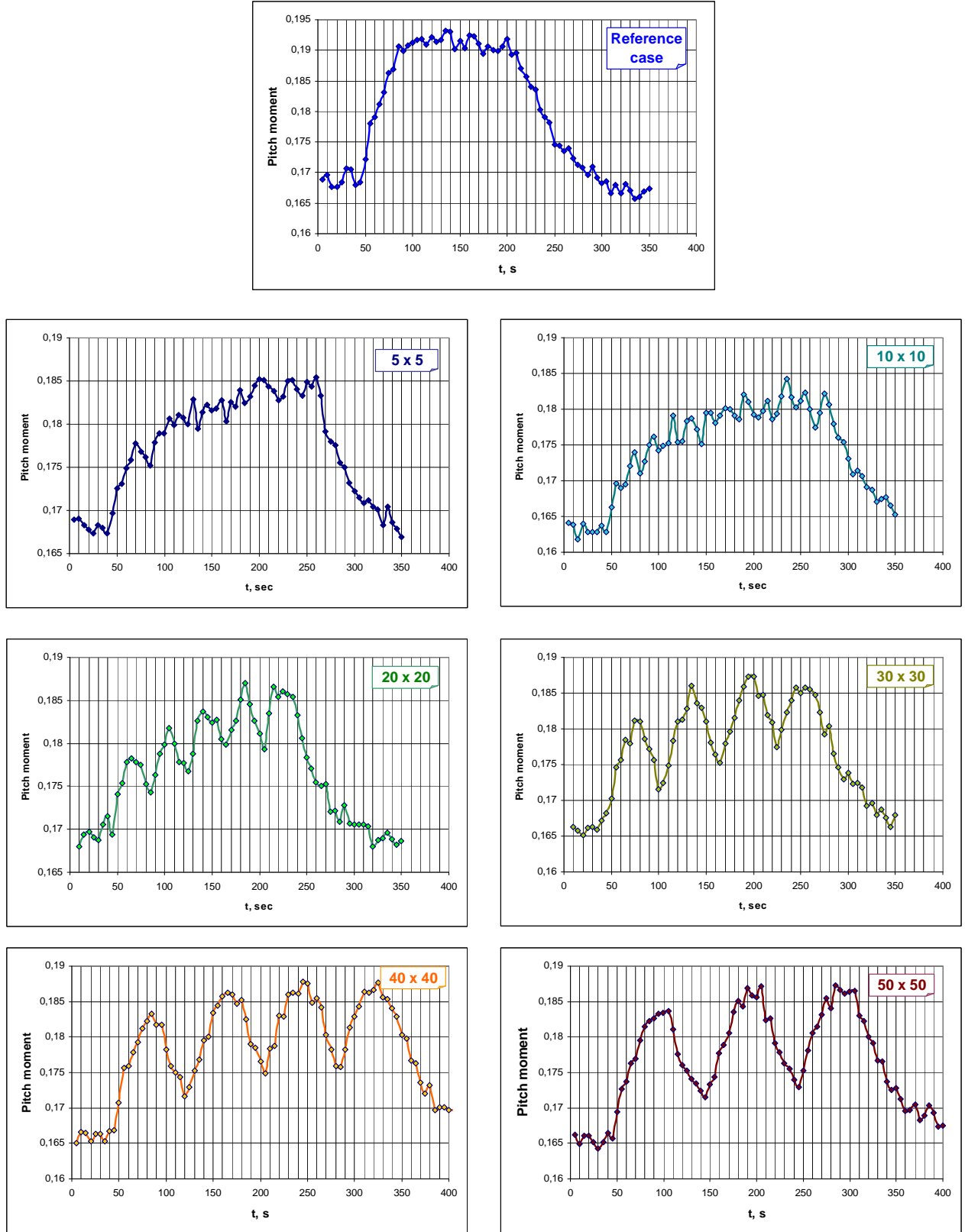


Fig. 3.3. Pitch moment coefficients for various modes of intermittent heating of sections S_3 and S_2 (Fig. 3.2) of the blade-type model R800 at its reverse position in the flow

measurement. The intermittent modes denoted as 5x5, 10x10, 20x20, etc. mean time intervals in seconds of the voltage switched on and off.

An influence of the thermal flow control intermittency can be guessed at the 5s x 5s mode becoming more and more apparent from 10s x 10s to 50s x 50s intervals. Greater intervals of periodic heating show a tendency of maximum values to approach those of the reference case. Besides, not completely cooled surface of the model during the voltage-off periods of time results in growth of these maximum values with time that is especially well seen for the 20s x 20s mode.

Thus it can be concluded that much greater frequencies in case of the pulse MW-initiated spanwise-regular thermal fields will not influence aerodynamic coefficients in a way shown in Fig.3.3. However non-stationary mechanisms can display themselves in a different way if a pulse mode will be used instead of continuous generation of z-regular plasma patches.

Comparative analysis of results obtained for the resistively heated model gave a guidance to design a plasma controlled model.

Design and fabrication of test models with plasma initiators

Test models with initiators for localized generation of plasma are designed so that on the one hand, to maintain maximum continuity with the earlier thermal flow control experiments, and on

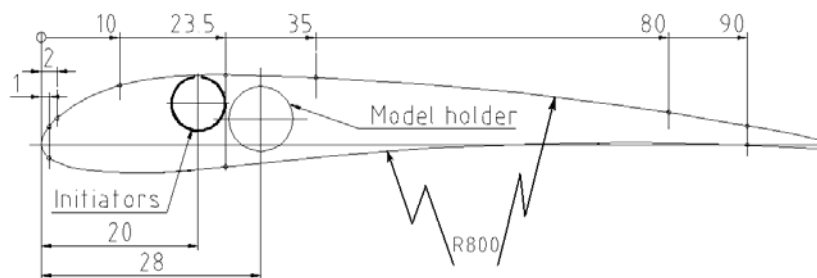


Fig. 3.4. Sketch of the model with plasma initiators: coordinates of drain ports are shown in percents of a chord

walls of 200 x 200 mm and the curvature radius $R=800$ mm. Relative thickness of the model of 0.12 as well as its leading and trailing parts were calculated to satisfy maximally the aerodynamic correctness of the airfoil design and at the same time, a possibility to locate the model in the flow back to front. The latter allows investigations both of a classical flow over a surface with constant curvature (reversed position) and of typical separation problems arising on turbine blades (forward position). It also enables more careful and correct comparative analysis of numerical and experimental results. Model fabrication is illustrated in Figs. 3.5.



Fig. 3.5. Fabrication of a model body according to the given geometry: the model with a holder within two moulds shaping convex and concave panels of the model.

Manufacturing of drained models with mounted pressure probes for local pressure measurements.

To realize the matching concept of experimental and numerical data, the drained model was designed with 14 surface pressure ports. Measured pressure variation over the model enables correct comparison and joint analysis of experimentally obtained aerodynamic coefficients and numeric pressure distributions over the model surface. Pressure ports are located at 7 downstream positions related to the cord, $X/c=1, 2, 10, 23.5, 35, 80$ and 90% along the convex surface and at $X/c=1, 35$ and 90% along the concave surface, while plasma initiators – at $X/c=20\%$ in the plane of symmetry of the model. Three spanwise groups of pressure ports are set at downstream positions of 23.5% and 35% of the cord so that the first port is located just downstream of the initiator tips, and the two lateral are at a spanwise distance of 1.25 and 2.5 mm from the first one. Ports 4, 5, 6 at $X/c=23.5\%$ are shown in Fig. 3.6; ports 7, 8, 9 are located similarly downstream, at $X/c=35\%$. The fabricated model with the pressure ports is shown in

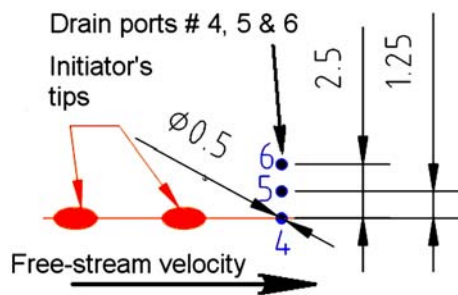


Fig. 3.6. Downstream layout of pressure ports

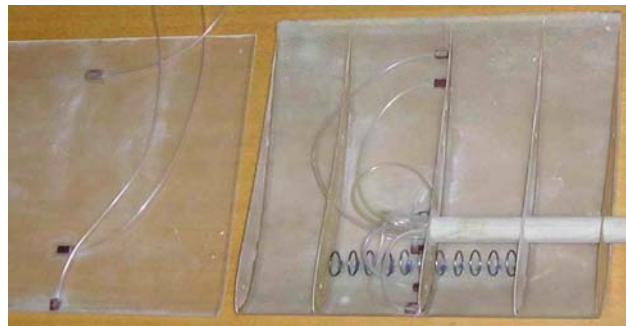


Fig. 3.7. Fabrication of the model with plasma initiators and drain ports for pressure measurements

Fig. 3.7. Embracing the model surface, probes enable to measure pressure fluctuations across the generated vortical structure: 3 lateral pressure probes cover $\frac{1}{4} \lambda_z$, where $\lambda_z = 10$ mm is a spanwise distance between MW initiators serving as a driving generator of a given turbulence scale in a boundary layer. If the initiator array causes the development of an adequate fluid motion scale, the discussed probes will give pressure values between generated streamwise vortices, along their core and in the middle.

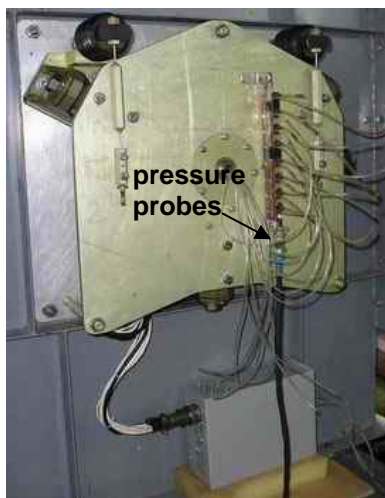


Fig. 3.8. Installed pressure probes

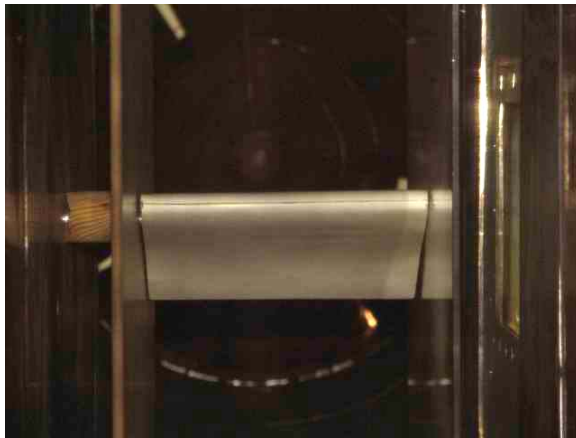
In the planned current tests, the discussed probe triplets were expected to provide necessary accuracy of static (stationary) pressure measurements.

Figures 3.7 and 3.8 illustrate respectively the internal view of preassembled model with the drainage and installation of pressure transducers on the strain gage. The bandwidth assessment of the pressure measurement system showed that pressure lag depends on both drain length and its diameter. The relevant procedure for getting amplitude-frequency characteristics was developed.

Requirements to the model materials are basically the same as earlier but supplemented with the requirement of radio-transparency:

- Low thermal conductivity and high dielectric properties of the basic (body) material to maintain a spanwise regular temperature gradient without uniform heating of the whole surface;

- Sufficiently high insulating and strength properties of a surface layer, its high-quality processing to provide a smooth surface;
- Long-term thermal resistance of the construction in localized areas of plasma initiators.
- Radio-transparency of all the model materials.



a) front view



b) side view

Fig. 3.9. Installation of models in the wind-tunnel test section

A set of samples of suitable materials was selected and tested under MW radiation and near-surface plasma generation with account of the mentioned requirements. As a result, it was concluded that foam plastic and cotton-based materials or a special kind of glass-bonded dielectric material were preferable to withstand the MW heating within operating times of the order of 1 s. In models with plasma initiators, series of holes are made at a selected chord position to mount ring-type plasma generators using heat-resistant cement. Ceramic insertions around plasma initiators provide durability of the model under high-temperature splashes in the vicinity of the model surface.

Fabricated models installed in the wind-tunnel test section are shown in Fig. 3.9.

Size and geometry of plasma initiators.

Aerodynamic requirements to plasma initiators are based on a possibility to have them flush-mounted in the model and spaced in a spanwise direction at 0.5-1.0 cm from each other. This is the MRTI part of research on a size and design elements related to the plug-in assembly of initiators taking into account their inevitable electrodynamic coupling. Ring-type initiators with a diameter of ~12 mm were chosen from the viewpoint of resonant interactions.

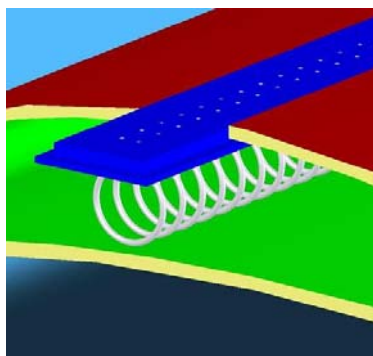


Fig. 3.10. Sketch of the plug-in assembly of initiators mounted in the model

The initiators plug-in assembly (Fig. 3.10) was fabricated as a plane strip 20 mm wide (streamwise) x 200 mm long (spanwise) x 3 mm thick (normal) using a micro-milling machine. It is mounted within the model body and adjusted to the model surface curvature ($R=800$ mm) to avoid surface roughness and, as a consequence, uncontrolled aerodynamic disturbances in a boundary layer. The plug-in assemblies are to be mounted both on concave and convex panels of the models to find their optimal location for flow control depending on basic flow parameters.

The technologically provided identity of the test models enables correct and accurate evaluation of flow control effects obtained on a small-size model under varying modes and intensity of various control factors. These factors, obeying the same flow-control strategy, can be realized using resistive or MW heating as well as MW-initiated plasma discharges. In addition, a number of variable control parameters are envisaged such as a downstream location of the control system, a spanwise scale of generated disturbances (a distance between neighboring plasma initiators or other heated elements) and a number of control plug-in assemblies in the model.

Initial runs with the plasma-actuator array in a wind tunnel showed its very unstable operation (Fig. 3.11): either not all the actuators generated plasma discharges or it was impossible to repeat the test under seemingly the same conditions. An obvious suggestion was made about a strongly nonuniform and unstable MW field within the wind tunnel test section. It was caused with multiple reflections and could be eliminated either using a more powerful MW generator or, if possible, operation in a standing wave mode.



Fig. 3.11. Pre-assembled model in the test section in a forward (a) and backward (b) positions

Thus prior aerodynamic measurements, appropriate organization of the MW energy flux within an extended area appeared to be a primary and most important problem to be solved in close cooperation with MRTI. Such tasks require numerous iterations to transfer the knowledge obtained in the MRTI desk-top facility into the full-scale IHM-NAU wind tunnel. These scale effects need thorough investigation together with guaranteed freedom of the model displacement within a range of angles of attack: sufficient amount of MW energy should be delivered to the model to enable the initiation of discharges.

Summary and test models used in the finalizing experiments

Altogether nine R800 models were designed and fabricated including reference (#0) and resistively heated (#1) models; #4 with embedded MW- heated elements is intended for the UKE2-1518 project. The Table below shows basic design features of the models used in plasma-control aerodynamic experiments; their detailed description is given in respective Progress Reports.

Summarized nomenclature and layout of R800 Models for UKE2-1508 Project

Model #	Initiators layout				Remarks
	Surface	Position, % of chord	Number	Step, mm	
2	convex	25	7	15	Feasibility check
3	convex	20	11	10	Initiators cover half span
6	convex	10	19	10	Full span, no discharges
7	convex	10.7	19	10	Initiators cover full span
5	concave	18.8	11	10	Initiators cover half span
8	concave	13.7	19	10	Initiators cover full span

All the models were tested under conditions of initiated plasma discharges except the model #6 which was unable to provide reliable stable discharges. Two #7 and #8 test models were thoroughly tested at the final stage of wind-tunnel experiments after the latest adjustments of the MW-generating system that is described in Chapter VII of this project.

Model #7 Layout

Model #7 has 19 initiators mounted on the convex (upper) surface with 10-mm spacing across the whole span of the model at the cordwise position of 21.30 mm from the leading edge, which corresponds to $\bar{x}_{init.} = 10.7\%$ of cord position. The model has 20 drain ports located as shown in Fig. 3.12. Drain ports 3, 5, 15, 21, and 23 were not connected. Model's chord is 198.7 mm and span is 200 mm with a holder located at $\bar{x}_h = 24,8\%$ of a cord position.

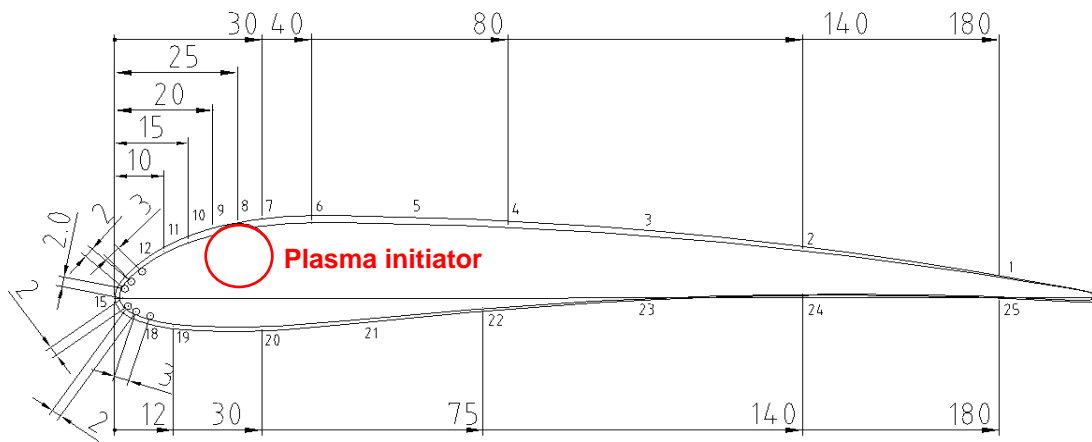


Fig. 3.12. Model #7 layout

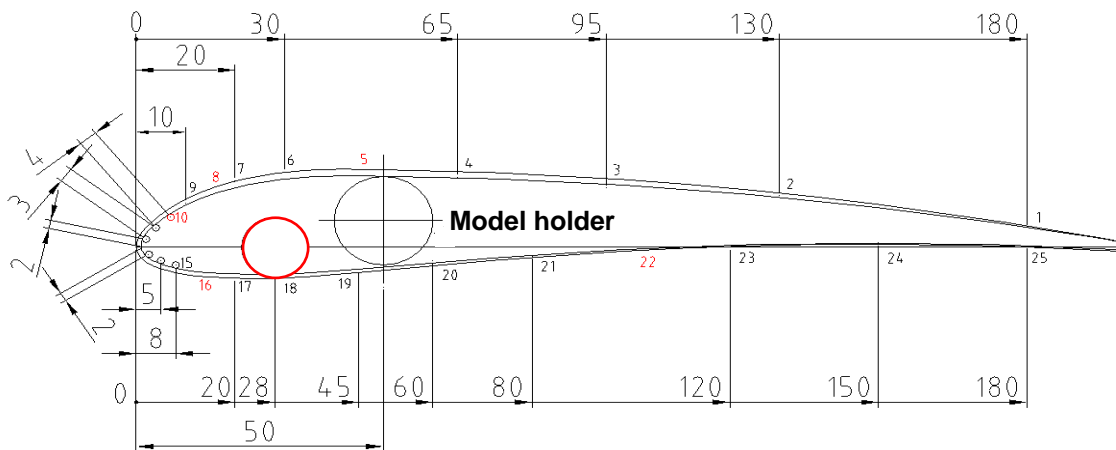


Fig. 3.13. Model #8 layout

Model #8 has 19 initiators mounted at 27 mm from the leading edge ($\bar{x}_{init.} = 13,70\%$ of the cord position) on the concave (lower) surface with a 10-mm step over the entire span of the model. Model has 20 drain ports shown in Fig. 3.13. Drain ports 5, 8, 10, 16, and 22 were not connected. Model has a chord of 197.1 mm and span of 200 mm with the holder located at $\bar{x}_h = 25,0\%$ of a cord position.

Both models have endplates 120 by 300 mm glued to left and right ribs of each model.

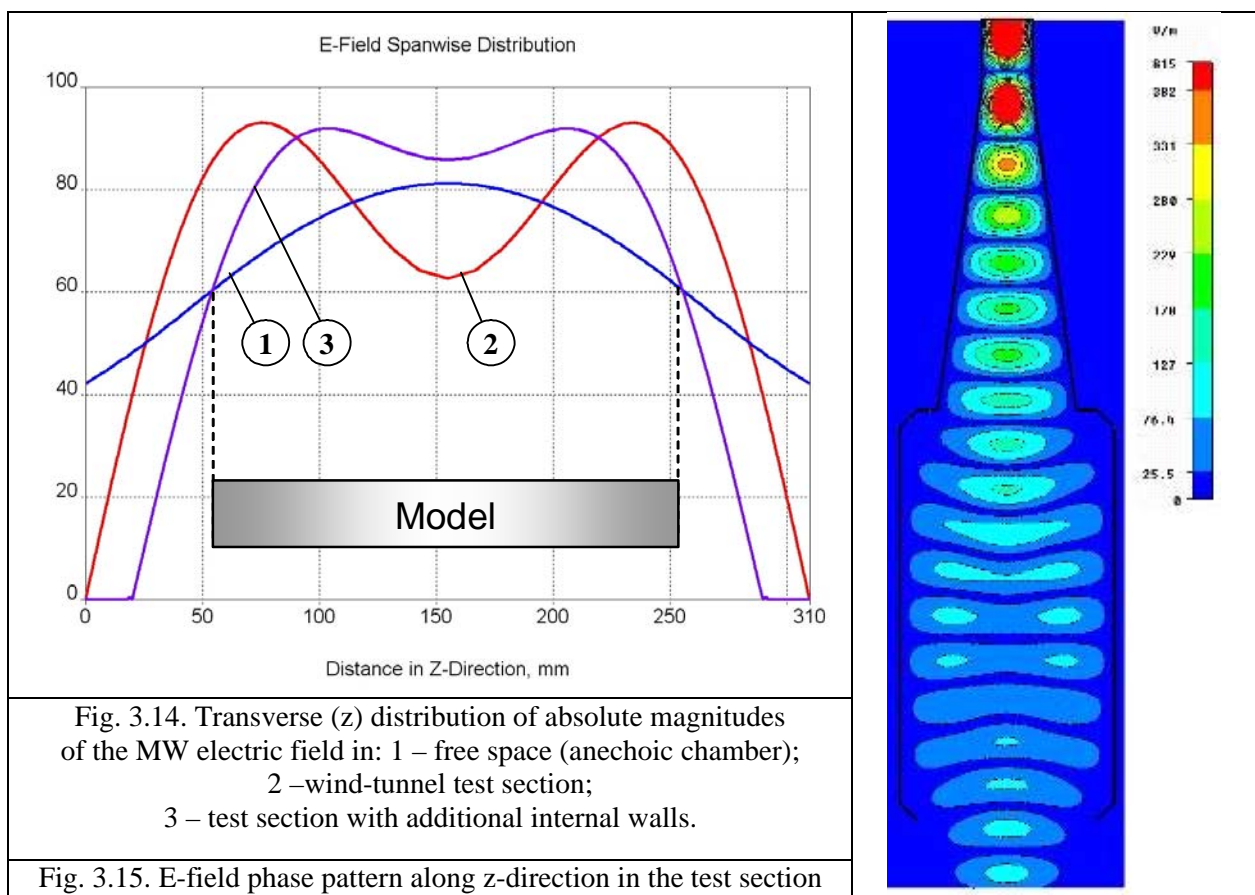
Finalized adjustments of electrodynamic and multi-initiator systems to wind-tunnel experimental conditions:

MRTI- NAU, Kiev

Optimization of the electrodynamic system, *MRTI*

Most recent numerical modeling of EM fields in the wind-tunnel test section showed the distribution displayed in Figs. 3.14 and 3.15. The geometry and sizes of the chamber in the 3D-model were taken to correspond exactly to a real test section of a wind tunnel in Kiev.

The left picture of Fig. 3.14 shows an unfavorable effect of metal walls of the chamber with its transversal dimension of 310 mm. At radiation wavelength of 12.24 cm and polarization of E vector parallel to the chamber side walls, they represent a waveguide electrodynamic system and directly impact on the EM field structure in transversely to the flow.



A typical bell-type field distribution in the free space (curve “1” in Fig. 3.14) is transformed to two-humped distribution with a strong sag along the chamber axis (curve “2”). This is also well seen in the phase field diagram of Fig. 3.15: the initially uniform phase front at the horn aperture is separated into two areas at the test model location.

For the best adjustment of the electrodynamic system to real wind-tunnel conditions, a full-scale analog of the wind-tunnel test section was manufactured in MRTI.

The analysis of modeling results taking into account real length of initiators system ~ 200 mm in spanwise direction (Fig. 3.14) shows that in this direction it is necessary to generate "a shelf" in the E (z) distribution. On the contrary, in a streamwise direction it is necessary to get

sharp focusing of MW radiation as a streamwise size of the initiator system is comparatively small.

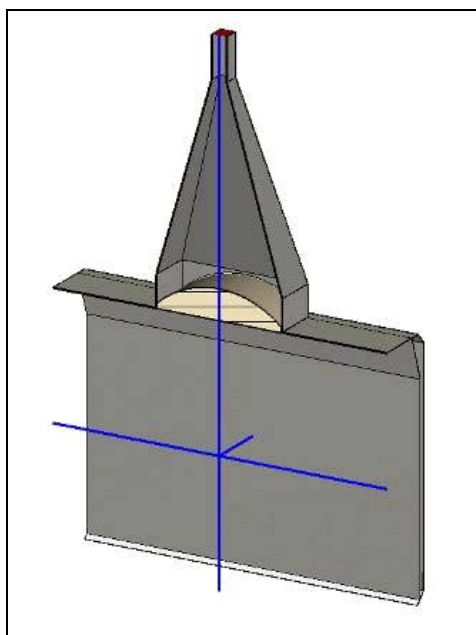


Fig. 3.16. Design based on a polythene focusing lens and additional metallic walls inside the wind-tunnel test section



Fig. 3.17. Newest irradiating horn with two polythene lenses inside

The first problem is solved using the installation of additional internal metal walls in the test section along a flow with the distance of 270-280 mm between them. However such an engineering solution should strictly correlate with aerodynamic requirements to parameters of the working section. Calculation results of an electromagnetic field for this design are presented in a form of curve “3” in Fig. 3.14.

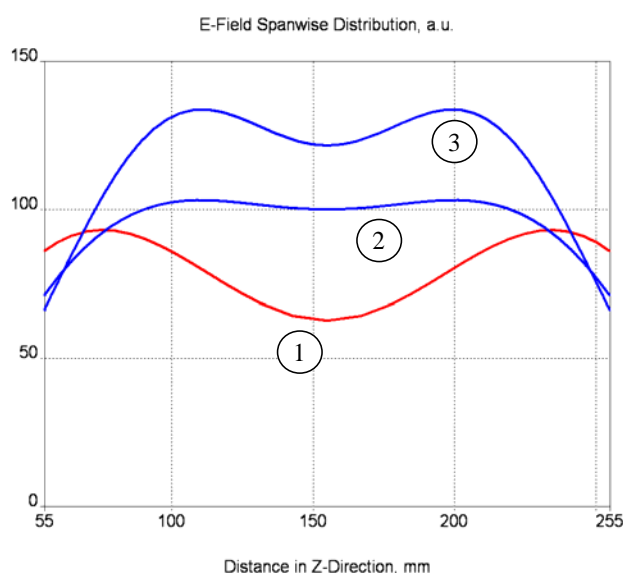


Fig. 3.18. Spanwise distribution of the E-field:
1 – initial test section; 2 – design with a polythene lens ($R = 220$ mm), 3 – design with a plate waveguide

Focusing of radiation along the streamwise X-axis appeared to be a more complicated task. At commensurability of MW radiation wavelength and dimensions of focusing elements, the efficiency of focusing is insignificant. Better focusing requires the ratio of the focusing lens diameter and the wavelength of EM field weeding no less than $D / \lambda = 6-10$, which is impossible for available dimensions of the wind-tunnel test section.

Two versions of the streamwise radiation focusing were considered and simulated numerically (details see in the 13-th QRT report on the project, paragraph 3.1):

(1) "Classical" case using a cylindrical dielectric lens in an opening of the radiating horn. This system is shown in Fig. 3.16, and the manufactured horn with the lenses - in Fig. 3.17.

(2) the original design based on "a lamellar waveguide», located in the test section above the model surface.

The first design does not need any explanations. The idea of the second one is considered in detail in paragraph 3.1 of the 13 QRT Report. The analysis of results of numerical modeling of both versions compared to the initial one (Fig. 3.18) confirmed that the efficiency of the second design was higher: the E-field in the area of initiators is visibly greater. However this design requires fulfillment of strict tolerances and is not so convenient in adjustments connected with the model attack of angle variations during the experiments. Therefore in practice, the choice was made in favour of a variant with focusing lenses.

The new horn (with the aperture 210×392 mm and height ~ 630 mm) with two polyethyleneflat-convex lenses (with the curvature radius ~ 270 mm) was manufactured, tested, delivered to Kiev and assembled in the IHM-NAU wind-tunnel facility before the final stage of aerodynamic experiments.

MW system modernization in the IHM-NAU wind tunnel and the airfoil model for full-scale aerodynamic experiments, NAU-MRTI

The newest progress of MRTI in the development of the MW system to provide stable generation of plasma discharges in the NAU-IHM wind tunnel and to be adjustable required the corresponding upgrade of the ACIR wind-tunnel equipment. It included installation of a new horn antenna with polyethylene lens to raise the MW power around the test model. For that, the opening on the upper wall of the Eiffel chamber was enlarged and an additional spacer unit was developed, manufactured, and mounted on the upper wall as it is shown in Fig. 3.19. In its turn, it required to enlarge the radio transparent window in the test-section upper wall because dimensions of the new antenna were greater than earlier.



Fig. 3.19. Horn antenna spacer unit

To obtain a more uniform distribution of electromagnetic field in the test area, a metal sheet was used in the test-section left wall to reflect EM field instead of its earlier organized absorption by the water-filled looking window (Fig. 3.20).

For the same purpose of energy saving, several configurations of the working area were tested including a flat metal sheet installed at distances of order of 2 – 5 cm above the lower test section wall. Besides, a cylindrical metal mirror was tried under the radio transparent lower wall of the test section. In addition, various streamwise locations of the horn antenna in a range of radiation power values were tested. Limitations of engineering solutions imposed by the available budget (e.g. the impossibility to purchase a more powerful magnetron) made a number of similar attempts unsuccessful or insufficiently effective. Finally, magnetron characteristics were analyzed and found to be lower in terms of the radiated power than it was documented. The new magnetron with the same rating power was free of this drawback.



Fig. 3.20. A metal reflector in the test section wall

The trial-and-error adjustments ended up with the following modifications of the MW system configuration and of relevant wind-tunnel parts.

- New magnetron, the newly designed horn antenna, the polyethylene lens mounted with the spacer unit.
- Test-section upper wall made from a flat metal sheet with a radio transparent window covered with a glass-fiber sheet.
- Flat metal bottom wall of the test section.
- Metal screen in the opening of the test section left-side wall.

The airfoil model with 19 initiators ($\lambda_z=10$ mm spacing) over a whole model span was tested in MRTI. Fig. 3.21, left shows a typical pattern of unstable discharges along the model span in the beginning of the concluding experiments. The situation is in a full agreement with the obtained numerical data (curve 2, Fig. 3.14).

Thorough adjustments of the electrodynamic system as well as of the test model according to the numerical recommendations resulted in the stable generation of all the 19 discharges covering the model span (Fig. 3.21, right) in the experimentally required range of angles of attack.



Fig. 3.21. Multiple MWdischarges in the vicinity of the airfoil model surface in wind-tunnel experiments: initial tests (left), and after the system adjustment (right)

Nevertheless, the fine tuning of a horn antenna position was necessary during the operation with each model to reach reliable plasma initiation; otherwise, it could happen that the initiation failed in the axial part of the model. The potential to improve the experimental system is far from being exhausted, e.g. the wind-tunnel test section can be narrowed to the value of 28 cm instead of the available 31 cm. But this and similar measures would require considerable efforts related to the modification of the wind-tunnel nozzle section.

MW-system operation, NAU-MRTI

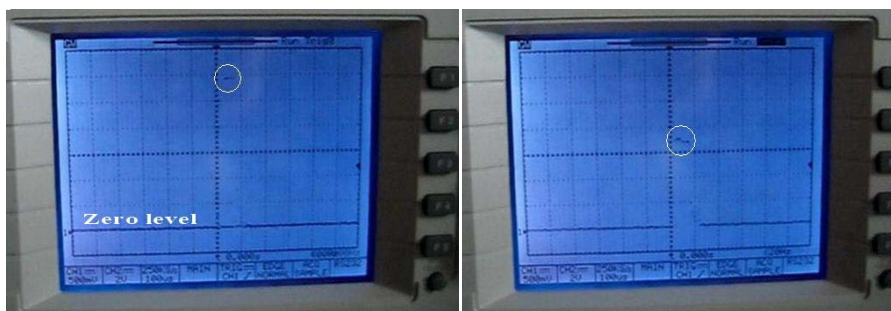


Fig. 3.22. Generated power drop within 1.3 s

It was found that the generated power dropped quickly after high voltage was switched on to feed the magnetron. Radiated power is proportional to magnetron current and this electric signal was connected to digital oscilloscope.

The system operation was designed for MW radiation in short pulses (50 – 100 μ s) with relatively

long intervals (600 – 900 μ s), so that mean power did not exceed 1 kW and off-duty factor was no more than 0.1. Fig. 3.22 shows two patterns made during model testing where a pulse position moves down within 1.3 sec. This means that at the end of a measuring period, the radiated power constitutes only 60% from its initial value. It is caused by the MW-system power supply, which has high-voltage single-phase transformer controlled by autotransformer with a limiter resistor to prevent its overload (see QRT7 UKE2-1508A-KV-05 progress report).

On the other hand, visual observations showed that discharges over the model remained stable and sometimes even better at the end of the measurement cycle.

Implementation of the atmosphere monitoring system, NAU

Analyzed experimental procedure, data processing and their presentation (see QTR13 UKE2-1508-KV-05 report) showed that the operation could be essentially improved due to the application of the “Troposphere-G” atmosphere monitoring system (AMS). It was purchased and integrated into the ACIR DAS. It enables simultaneous measurements of barometric pressure, air temperature and humidity with the documented errors: 0.3 mm hg for barometric pressure, 0.2°C for temperature, and 2% for relative humidity. This DAS optimization reduces an error of air density measurement to the level of 0.08% and connected errors of free-stream velocity measurements to the level of 0.04%. A combined error of calculated kinematic viscosity is 0.16%.

AMS is equipped with RS-232 interface connected to COM-2 port of DAS. Test software was modified accordingly so that atmosphere parameters were measured at each particular angle of attack just before measurements of loads and pressures during test runs instead of their manual keyboard input in the beginning of a test run.

Due to the application of the new system, air density variations during a test run could be registered up to the value of 0.002 kg/m³ or 0.17%.